Cite as: W. Yao *et al.*, *Science* 10.1126/science.aar8658 (2018).

Large-scale ocean deoxygenation during the Paleocene-Eocene Thermal Maximum

Weiqi Yao[1]*, Adina Paytan[2], Ulrich G. Wortmann[1]

[1]Department of Earth Sciences, University of Toronto, Toronto, Ontario, M5S 3B1, Canada. [2]Institute of Marine Science, University of California–Santa Cruz, Santa Cruz, CA 95064, USA.

*Corresponding author. E-mail: weiqi.yao@mail.utoronto.ca

The consequences of global warming for fisheries are not well understood, but the geological record demonstrates that carbon cycle perturbations are frequently associated with ocean deoxygenation. Of particular interest is the Paleocene-Eocene Thermal Maximum (PETM) where the CO_2 input into the atmosphere was similar to the IPCC RCP8.5 emission scenario. Here we present sulfur-isotope data which record a positive 1 ‰ excursion during the PETM. Modeling suggests that significant parts of the ocean must have become sulfidic. The toxicity of hydrogen sulfide will render two of the largest and least explored ecosystems on Earth, the mesopelagic and bathypelagic zones, uninhabitable by multi-cellular organisms. This will affect many marine species whose eco-zones stretch into the deep ocean.

The geological record contains many examples in which the earth system was out of equilibrium and large parts of the ocean were inhospitable to life. However, only few of these events can provide insight about the effects of modern fossil fuel burning. This is because either the boundary conditions are substantially different (e.g., the plate-tectonic configuration) or the rate of change is not comparable. The short-lived PETM event (~55 Ma) (*1*) is a notable exception. Current data suggest that in the PETM the atmosphere had to accommodate about 2500-4500 Gt of carbon released within 4000 years (*2*). This is an increase of the same order of magnitude as the IPCC RCP8.5 emission scenario, which projects a cumulative anthropogenic CO_2 release of 2000 GtC by 2100 (*3*). Although the carbon dioxide release rate during the PETM was about 10 times slower, it is our best analog to study non-linear feedbacks and consequences of the anthropogenic carbon cycle perturbation.

The geochemical cycles of carbon and sulfur are linked through microbial sulfate reduction (MSR), where the electron transfer from sulfate to sulfide provides the energy to respire organic matter (OM) back to CO_2. Combined, these cycles constitute the dominant control on atmospheric oxygen (*4*, *5*). Due to their drastically different residence times (0.1 Myrs versus 10 Myrs) (*4*), they are rarely considered together. Our data suggest however that MSR is able to alter the redox state of the marine sulfur reservoir on timescales which are comparable to that of the carbon cycle. This has three important implications: 1) Unlike oxic respiration MSR also produces H_2S which is toxic to most life forms even at low concentrations; 2) If we accept the premise that the PETM is a model for the present day oceans, the timescales of the observed changes in the redox state of marine sulfur suggest that similar processes could affect the oceans in the near future; 3) The development of oxygen free waters creates a sizable but intermittent reservoir in the global sulfur cycle, with fluxes exceeding traditional weathering/burial flux estimates.

The mass and sulfur isotope ratio of seawater sulfate are controlled by sulfur delivered to the oceans via weathering and volcanic degassing and sulfur removed from the oceans via burial of sulfur-bearing minerals. In marine sediments, sulfur is present in its oxidized form as sulfate-bearing evaporite salts and in its reduced state as metal sulfides. Sulfate-bearing evaporites precipitate with little or no fractionation relative to seawater, and thus have a limited effect on the S-isotope ratio of seawater sulfate (*5*, *6*). In contrast, MSR has a preference for ^{32}S, and thus exerts a significant influence on the seawater $^{34}S/^{32}S$ ratio (*7*, *8*). In this study, we use pristine authigenic marine barite crystals to trace the evolution of the marine S-isotope ratio across the PETM. We report our results in the traditional delta notation ($\delta^{34}S$) which expresses the isotopic ratio of $^{34}S/^{32}S$ as a difference relative to a reference standard:

$$\delta^{34}S = \frac{\left(\frac{^{34}S}{^{32}S}\right)_{Sample} - \left(\frac{^{34}S}{^{32}S}\right)_{Standard}}{\left(\frac{^{34}S}{^{32}S}\right)_{Standard}} \times 1000\ [‰]$$

where ^{x}S denotes the concentration of the respective sulfur isotope. All results are reported relative to the Vienna Canyon Diabolo Troillite (VCDT).

We observe a 1 ‰ shift in $\delta^{34}S$ during the PETM (Fig. 1) which implies the removal of 8×10^{16} moles of reduced sulfur within 50 kyrs from the oceans (assuming a marine sulfate

Downloaded from http://science.sciencemag.org/ on July 19, 2018

concentration of 5 mM) (*9*). This requires more than double the pre-PETM steady-state pyrite burial flux. Even more surprising is the fast decay of the S-isotope excursion, which occurs within approximately 100 kyrs. Due to the large size of the marine sulfate reservoir and the small input/output fluxes to the ocean, the marine S-isotope ratio is expected to retain the peak S-isotope values of the excursion for millions of years before returning to pre-excursion conditions. The observed rapid decay of the S-isotope excursion requires the input of 8×10^{16} moles of isotopically light sulfur back into the ocean before the end of the PETM.

Changes in pyrite burial are traditionally invoked to explain changes in seawater $\delta^{34}S$. It is assumed that most of the pyrite burial happens on continental shelves (*10*, *11*). As such, pyrite burial rates correlate with sea level variations, i.e., during high stands, shelf areas expand and pyrite burial increases, whereas during low stands shelf areas shrink and previously buried pyrite is re-oxidized (*11*). Sea-level estimates suggest a rise on the order of 25 m during the PETM (*12*). Using previously published parametrizations (*11*) this results in the additional burial of 4.45×10^{10} mol pyrite per year, about 4% of that required to explain the observed isotope shift. The idea that the shelf acts as a transient pyrite reservoir has been expressed previously (*11*, *13*) but the observed isotope signal requires an increase of the global shelf area equivalent to 13-32 times the size of the contiguous United States. Clearly, these numbers depend on a variety of assumptions, chiefly, the OM and pyrite burial rates on the shelves, however, they do demonstrate the magnitude of required flux changes.

Previous authors proposed that the importance of continental shelves for pyrite burial may have been overstated (*11*, *14*) and that the long-term burial of pyrite is controlled by the intensity of anaerobic methane oxidation (AMO) on continental slopes (*14*). This idea is particularly intriguing because it links pyrite burial to sub-seafloor methane flux, which in turn has been suggested as a possible explanation for the negative carbon isotope excursion in the PETM (*14*, *15*). In this scenario, the rapid release of isotopically light methane would not only drive the observed C-cycle excursion but also increase pyrite burial rates.

Linking pyrite burial flux to methane flux is elegant and provides a plausible explanation for the rise in the marine $\delta^{34}S$ ratio during the PETM. Furthermore, once the methane has been vented, gas hydrate reservoirs will have to recharge and thus AMO fluxes and AMO associated pyrite burial rates will cease (*14*). However, even if we assume the extreme case that all pyrite burial is AMO-controlled, it would take at least 0.2 Myrs to return the marine $\delta^{34}S$ ratio back to its pre-excursion value (see Supplementary Materials). In other words, it is not sufficient just to inhibit all pyrite burial; rather, we need to inject large quantities of isotopically light S into the oceans in order to explain the observed S-isotope signal. The speed and magnitude of the required ^{32}S flux require a transient reservoir of ^{32}S enriched sulfur which is sufficiently large to hold 8×10^{16} mol of isotopically depleted S and can be charged and released in less than 100 kyrs.

Here we propose that the marine oxygen minimum zone (OMZ) constitutes such a reservoir. With the exception of a few upwelling zones, oxygen levels in the OMZ are usually high enough to render MSR energetically unfavorable. However, the marine oxygen pool is small and changes in circulation or export production can alter the oxygen content of the OMZ rapidly. Once oxygen levels in the OMZ drop below 4 μM (*16*), MSR becomes the dominant OM remineralization pathway. In the modern ocean, MSR is limited by OM supply and the diffusive supply of sulfate into the sediment column. Shifting the location of sulfate reduction from the sediment into the intermediate water column, we not only increase the availability of sulfate, but drastically increase the quality and quantity of OM. This will accelerate the globally integrated sulfate reduction flux and transfer ^{32}S into the OMZ, effectively separating the ocean into two sulfur reservoirs.

To estimate the required changes to the OMZ, we use S-isotope fractionation factors (α) between 43 ‰ and 70 ‰ (*7*, *8*), and an average sulfide concentration to 0.5 mM, well below the 1 mM threshold where chemocline upwelling and the subsequent release of H_2S into the atmosphere become a possibility (*17*). The value of 0.5 mM is high compared to sulfide concentrations observed in anoxic upwelling zones in the modern ocean (*16*), but well within the limits of marine sulfide concentrations observed within more restricted settings (e.g., 6.14 mM in Framvaren Fjord) (*18*). Modeling the data using the statistically significant maximum of 18.35 ‰ (Fig. 2), requires sulfidic water volumes between 1.6×10^{17} to 2.6×10^{17} m^3. The highest measured $\delta^{34}S$ value (18.95 ‰), can be explained with a sulfidic water volume of no more than 2.7×10^{17} m^3 for α of 70 ‰. To put these estimates into perspective: In the modern ocean, the OMZ sensu stricto (O_2 < 20 μM) encompasses about 1% of the global ocean volume (1.38×10^{18} m^3) (*19*), whereas the above numbers suggest an order of magnitude increase to 10-20% of the ocean volume. Several studies indeed suggest that low-O_2 or anoxic waters were present during the PETM at intermediate depths in many ocean basins (*20–23*).

Modeling predictions exploring the effects of antrophogenic climate change suggest that measurable oxygen loss from the subarctic North Pacific will occur by 2030-2040 (*24*) and that the total volume of suboxic ocean water will expand by 50% by 2100 (*25*). Once local oxygen concentrations drop below 4 μM (*16*), sulfate reduction will commence, resulting in the production of H_2S, which is toxic at levels as low as 4 μg/l (*26*). This will: A) Create an ocean internal reservoir of reduced sulfur; B) Create and ocean which is no longer well

Downloaded from http://science.sciencemag.org/ on July 19, 2018

mixed with respect to sulfate; C) Compress the eco-zones of fish species which venture in the mesopelagic and bathypelagic zones (*27*) and change their ecosystem structure which could jeopardize 10-50% of worldwide pelagic predator diversity (*27*) with unknown consequences for global fish stocks. Our findings suggest that A and B have been well expressed during the PETM, and given the similarities between the PETM and the IPCC RCP8.5 emission scenario, C will be a possibility in the not too distant future.

REFERENCES AND NOTES

1. F. Nunes, R. Norris, in *Proceedings of the Ocean Drilling Program, Scientific Results*, P. Wilson, M. Lyle, J. Firth, Eds. (College Station, TX, 2005), vol. 199, pp. 1–12.
2. R. Zeebe, A. Ridgwell, J. Zachos, Anthropogenic carbon release rate unprecedented during the past 66 million years. *Nat. Geosci.* **9**, 325–329 (2016). doi:10.1038/ngeo2681
3. "IPCC, *Climate Change 2013: The Physical Science Basis. Contribution of Working Group I to the Fifth Assessment Report of the Intergovernmental Panel on Climate Change*, T. F. Stocker *et al*., Eds. (Cambridge Univ. Press, 2013).
4. J. C. Walker, Global geochemical cycles of carbon, sulfur and oxygen. *Mar. Geol.* **70**, 159–174 (1986). doi:10.1016/0025-3227(86)90093-9 Medline
5. U. G. Wortmann, B. M. Chernyavsky, Effect of evaporite deposition on Early Cretaceous carbon and sulphur cycling. *Nature* **446**, 654–656 (2007). doi:10.1038/nature05693 Medline
6. G. Claypool, W. Holser, I. Kaplan, H. Sakai, I. Zak, The age curves of sulfur and oxygen isotopes in marine sulfate and their mutual interpretation. *Chem. Geol.* **28**, 199–260 (1980). doi:10.1016/0009-2541(80)90047-9
7. I. Kaplan, K. Emery, S. Rittenberg, The distribution and isotopic abundance of sulphur in recent marine sediments off southern California. *Geochim. Cosmochim. Acta* **27**, 297–331 (1963). doi:10.1016/0016-7037(63)90074-7
8. U. Wortmann, S. Bernasconi, M. Böttcher, Hypersulfidic deep biosphere indicates extreme sulfur isotope fractionation during single-step microbial sulfate reduction. *Geology* **29**, 647–650 (2001). doi:10.1130/0091-7613(2001)029<0647:HDBIES>2.0.CO;2
9. U. G. Wortmann, A. Paytan, Rapid variability of seawater chemistry over the past 130 million years. *Science* **337**, 334–336 (2012). doi:10.1126/science.1220656 Medline
10. A. Turchyn, D. Schrag, Cenozoic evolution of the sulfur cycle: Insight from oxygen isotopes in marine sulfate. *Earth Planet. Sci. Lett.* **241**, 763–779 (2006). doi:10.1016/j.epsl.2005.11.007
11. S. Markovic, A. Paytan, U. Wortmann, Pleistocene sediment offloading and the global sulfur cycle. *Biogeosciences* **12**, 3043–3060 (2015). doi:10.5194/bg-12-3043-2015
12. K. G. Miller, M. A. Kominz, J. V. Browning, J. D. Wright, G. S. Mountain, M. E. Katz, P. J. Sugarman, B. S. Cramer, N. Christie-Blick, S. F. Pekar, The Phanerozoic record of global sea-level change. *Science* **310**, 1293–1298 (2005). doi:10.1126/science.1116412 Medline
13. J. Higgins, D. Schrag, Beyond methane: Towards a theory for the Paleocene–Eocene Thermal Maximum. *Earth Planet. Sci. Lett.* **245**, 523–537 (2006). doi:10.1016/j.epsl.2006.03.009
14. G. Dickens, Down the Rabbit Hole: Toward appropriate discussion of methane release from gas hydrate systems during the Paleocene-Eocene thermal maximum and other past hyperthermal events. *Clim. Past* **7**, 831–846 (2011). doi:10.5194/cp-7-831-2011
15. G. Dickens, J. O'Neil, D. Rea, R. Owen, Dissociation of oceanic methane hydrate as a cause of the carbon isotope excursion at the end of the Paleocene. *Paleoceanography* **10**, 965–971 (1995). doi:10.1029/95PA02087
16. V. Brüchert, B. B. Jørgensen, K. Neumann, D. Riechmann, M. Schlösser, H. Schulz, Regulation of bacterial sulfate reduction and hydrogen sulfide fluxes in the central namibian coastal upwelling zone. *Geochim. Cosmochim. Acta* **67**, 4505–4518 (2003). doi:10.1016/S0016-7037(03)00275-8
17. L. Kump, A. Pavlov, M. Arthur, Massive release of hydrogen sulfide to the surface ocean and atmosphere during intervals of oceanic anoxia. *Geology* **33**, 397–400 (2005). doi:10.1130/G21295.1
18. W. Landing, S. Westerlund, The solution chemistry of iron(II) in Framvaren Fjord. *Mar. Chem.* **23**, 329–343 (1988). doi:10.1016/0304-4203(88)90102-8
19. A. Paulmier, D. Ruiz-Pino, Oxygen minimum zones (OMZs) in the modern ocean. *Prog. Oceanogr.* **80**, 113–128 (2009). doi:10.1016/j.pocean.2008.08.001
20. M. Nicolo, G. Dickens, C. Hollis, South Pacific intermediate water oxygen depletion at the onset of the Paleocene-Eocene thermal maximum as depicted in New Zealand margin sections. *Paleoceanography* **25**, PA4210 (2010). doi:10.1029/2009PA001904
21. A. Dickson, A. Cohen, A. Coe, Seawater oxygenation during the Paleocene-Eocene Thermal Maximum. *Geology* **40**, 639–642 (2012). doi:10.1130/G32977.1
22. A. Winguth, E. Thomas, C. Winguth, Global decline in ocean ventilation, oxygenation, and productivity during the Paleocene-Eocene Thermal Maximum: Implications for the benthic extinction. *Geology* **40**, 263–266 (2012). doi:10.1130/G32529.1
23. X. Zhou, E. Thomas, A. M. E. Winguth, A. Ridgwell, H. Scher, B. A. A. Hoogakker, R. E. M. Rickaby, Z. Lu, Expanded oxygen minimum zones during the late Paleocene-early Eocene: Hints from multiproxy comparison and ocean modeling. *Paleoceanography* **31**, 1532–1546 (2016). doi:10.1002/2016PA003020
24. M. C. Long, C. Deutsch, T. Ito, Finding forced trends in oceanic oxygen. *Global Biogeochem. Cycles* **30**, 381–397 (2016). doi:10.1002/2015GB005310
25. A. Oschlies, K. Schulz, U. Riebesell, A. Schmittner, Simulated 21st century's increase in oceanic suboxia by CO_2-enhanced biotic carbon export. *Global Biogeochem. Cycles* **22**, GB4008 (2008). doi:10.1029/2007GB003147
26. L. Smith, D. Oseid, I. Adelman, S. Broderius, Effect of hydrogen sulfide on fish and invertebrates. Part I – Acute and chronic toxicity studies. *Ecol. Res. Tech. Rep. Ser. No.3* (U.S. Environmental Protection Agency, 1976).
27. L. Stramma, E. D. Prince, S. Schmidtko, J. Luo, J. P. Hoolihan, M. Visbeck, D. W. R. Wallace, P. Brandt, A. Körtzinger, Expansion of oxygen minimum zones may reduce available habitat for tropical pelagic fishes. *Nat. Clim. Chang.* **2**, 33–37 (2012). doi:10.1038/nclimate1304
28. J. Zachos *et al*., *Proceedings of the Ocean Drilling Program, Initial Reports* (College Station, Texas, 2004), vol. 208, pp. 1–112.
29. T. Coplen *et al.*, *Compilation of minimum and maximum isotope ratios of selected elements in naturally occurring terrestrial materials and reagents*. U.S. *Geological Survey Water-Resources Investigations Report*, 01–4222 (2001).
30. S. Henkel, J. M. Mogollón, K. Nöthen, C. Franke, K. Bogus, E. Robin, A. Bahr, M. Blumenberg, T. Pape, R. Seifert, C. März, G. J. de Lange, S. Kasten, Diagenetic barium cycling in Black Sea sediments – A case study for anoxic marine environments. *Geochim. Cosmochim. Acta* **88**, 88–105 (2012). doi:10.1016/j.gca.2012.04.021
31. A. Paytan, S. Mearon, K. Cobb, M. Kastner, *Geol. Soc. Am.* **30**, 747–750 (2002).
32. E. Griffith, E. Schauble, T. Bullen, A. Paytan, Characterization of calcium isotopes in natural and synthetic barite. *Geochim. Cosmochim. Acta* **72**, 5641–5658 (2008). doi:10.1016/j.gca.2008.08.010
33. E. Griffith, M. Fantle, A. Eisenhauer, A. Paytan, T. Bullen, Effects of ocean acidification on the marine calcium isotope record at the Paleocene–Eocene Thermal Maximum. *Earth Planet. Sci. Lett.* **419**, 81–92 (2015). doi:10.1016/j.epsl.2015.03.010
34. A. Paytan, M. Kastner, E. Martin, J. Macdougall, T. Herbert, Marine barite as a monitor of seawater strontium isotope composition. *Nature* **366**, 445–449 (1993). doi:10.1038/366445a0
35. A. Paytan, K. Averyt, K. Faul, E. Gray, E. Thomas, *Geol. Soc. Am.* **35**, 1139–1142 (2007).
36. D. Hodell, G. D. Kamenov, E. C. Hathorne, J. C. Zachos, U. Röhl, T. Westerhold, Variations in the strontium isotope composition of seawater during the Paleocene and early Eocene from ODP Leg 208 (Walvis Ridge). *Geochem. Geophys. Geosyst.* **8**, Q09001 (2007). doi:10.1029/2007GC001607
37. W. Cleveland, Robust Locally Weighted Regression and Smoothing Scatterplots. *J. Am. Stat. Assoc.* **74**, 829–836 (1979). doi:10.1080/01621459.1979.10481038
38. R Core Team, R: *a language and environment for statistical computing*, R Foundation. for Statistical Computing (Vienna, Austria, 2012).
39. J. C. Zachos, U. Röhl, S. A. Schellenberg, A. Sluijs, D. A. Hodell, D. C. Kelly, E. Thomas, M. Nicolo, I. Raffi, L. J. Lourens, H. McCarren, D. Kroon, Rapid acidification of the ocean during the Paleocene-Eocene thermal maximum.

Downloaded from http://science.sciencemag.org/ on July 19, 2018

Science **308**, 1611–1615 (2005). doi:10.1126/science.1109004 Medline
40. U. Röhl, T. Bralower, R. Norris, G. Wefer, New chronology for the late Paleocene thermal maximum and its environmental implications. *Geology* **28**, 927–930 (2000). doi:10.1130/0091-7613(2000)28<927:NCFTLP>2.0.CO;2
41. T. Ding, S. Valkiers, H. Kipphardt, P. De Bièvre, P. D. P. Taylor, R. Gonfiantini, R. Krouse, Calibrated sulfur isotope abundance ratios of three IAEA sulfur isotope reference materials and V-CDT with a reassessment of the atomic weight of sulfur. *Geochim. Cosmochim. Acta* **65**, 2433–2437 (2001). doi:10.1016/S0016-7037(01)00611-1
42. R. Garrel, A. Lerman, Coupling of the sedimentary sulfur and carbon cycles; an improved model. *Am. J. Sci.* **284**, 989–1007 (1984). doi:10.2475/ajs.284.9.989
43. L. Kump, R. Garrels, Modeling atmospheric O_2 in the global sedimentary redox cycle. *Am. J. Sci.* **286**, 337–360 (1986). doi:10.2475/ajs.286.5.337
44. A. Kurtz, L. Kump, M. Arthur, J. Zachos, A. Paytan, Early Cenozoic decoupling of the global carbon and sulfur cycles. *Paleoceanography* **18**, 1090–1103 (2003). doi:10.1029/2003PA000908
45. S. Bottrell, R. Newton, Reconstruction of changes in global sulfur cycling from marine sulfate isotopes. *Earth Sci. Rev.* **75**, 59–83 (2006). doi:10.1016/j.earscirev.2005.10.004
46. R. Berner, Burial of organic carbon and pyrite sulfur in the modern ocean; its geochemical and environmental significance. *Am. J. Sci.* **282**, 451–473 (1982). doi:10.2475/ajs.282.4.451
47. B. Jørgensen, Mineralization of organic matter in the sea bed—The role of sulphate reduction. *Nature* **296**, 643–645 (1982). doi:10.1038/296643a0
48. M. Jacobsen, R. Charlson, H. Rodhe, G. Orians, *Earth System Science: From Biogeochemical Cycles to Global Change* (Elsevier, Amsterdam, 2000).
49. D. Canfield, Biogeochemistry of sulfur isotopes. *Rev. Mineral. Geochem.* **43**, 607–636 (2001). doi:10.2138/gsrmg.43.1.607
50. M. Rudnicki, H. Elderfield, B. Spiro, Fractionation of sulfur isotopes during bacterial sulfate reduction in deep ocean sediments at elevated temperatures. *Geochim. Cosmochim. Acta* **65**, 777–789 (2001). doi:10.1016/S0016-7037(00)00579-2
51. B. Chernyavsky, U. Wortmann, REMAP: A reaction transport model for isotope ratio calculations in porous media. *Geochem. Geophys. Geosyst.* **8**, Q02009 (2007). doi:10.1029/2006GC001442
52. L. Legendre, Flux of particulate organic material from the euphotic zone of oceans: Estimation from phytoplankton biomass. *J. Geophys. Res.* **103**, 2897–2903 (1998). doi:10.1029/97JC02706
53. Z. Ma, E. Gray, E. Thomas, B. Murphy, J. Zachos, A. Paytan, Carbon sequestration during the Palaeocene–Eocene Thermal Maximum by an efficient biological pump. *Nat. Geosci.* **7**, 382–388 (2014). doi:10.1038/ngeo2139
54. K. Burke, A. Sengör, Ten metre global sea-level change associated with South Atlantic Aptian salt deposition. *Mar. Geol.* **83**, 309–312 (1988). doi:10.1016/0025-3227(88)90064-3
55. A. Paytan, M. Kastner, D. Campbell, M. H. Thiemens, Sulfur isotopic composition of cenozoic seawater sulfate. *Science* **282**, 1459–1462 (1998). doi:10.1126/science.282.5393.1459 Medline
56. J. Horita, H. Zimmermann, H. Holland, Chemical evolution of seawater during the Phanerozoic. *Geochim. Cosmochim. Acta* **66**, 3733–3756 (2002). doi:10.1016/S0016-7037(01)00884-5
57. K. Hansen, K. Wallman, Cretaceous and Cenozoic evolution of seawater composition, atmospheric O2 and CO2: A model perspective. *Am. J. Sci.* **303**, 94–148 (2003). doi:10.2475/ajs.303.2.94
58. S. Petsch, R. Berner, Coupling the geochemical cycles of C, P, Fe, and S; the effect on atmospheric O_2 and the isotopic records of carbon and sulfur. *Am. J. Sci.* **298**, 246–262 (1998). doi:10.2475/ajs.298.3.246

ACKNOWLEDGMENTS

We thank G.R. Dickens and S. Markovic for discussions and comments on an early draft of this paper, H. Li for her support with the isotope analysis, and the three anonymous reviewers for helping to improve this manuscript. **Funding:** This research was supported by a Discovery Grant of the Natural Sciences and Engineering Research Council of Canada (NSERC) to U.G.W. and a National Science Foundation (NSF) CAREER grant OCE-0449732 to A.P. **Author contributions:** All authors contributed to the ideas expressed in this manuscript. W.Y. and U.G.W. developed the project. A.P. provided barite samples. W.Y. performed isotope measurements, data analysis, computations and did the art work. W.Y., U.G.W. and A.P. were responsible for data interpretation and manuscript writing. **Competing interests:** The authors declare no competing interest. **Data and materials availability:** All data are available in Supplementary Materials.

SUPPLEMENTARY MATERIALS

www.sciencemag.org/cgi/content/full/science.aar8658/DC1
Materials and Methods
Figs. S1 to S8
Tables S1 and S2
References (*28*–*58*)

27 December 2017; accepted 7 July 2018
Published online 19 July 2018
10.1126/science.aar8658

Downloaded from http://science.sciencemag.org/ on July 19, 2018

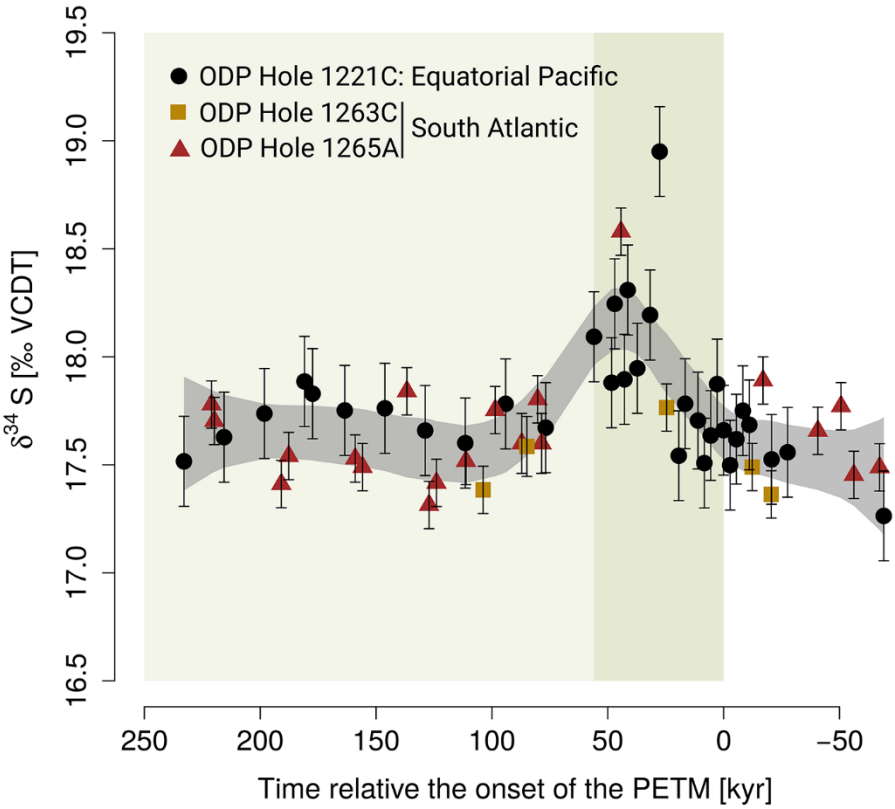

Fig. 1. $\delta^{34}S$ data of authigenic marine barite crystals across the PETM. The grey area denotes the 95% confidence interval of the LOESS regression (see Supplementary Materials). Shaded boxes indicate the extents of the main and total PETM interval (1). Error bars are 1-σ.

Downloaded from http://science.sciencemag.org/ on July 19, 2018

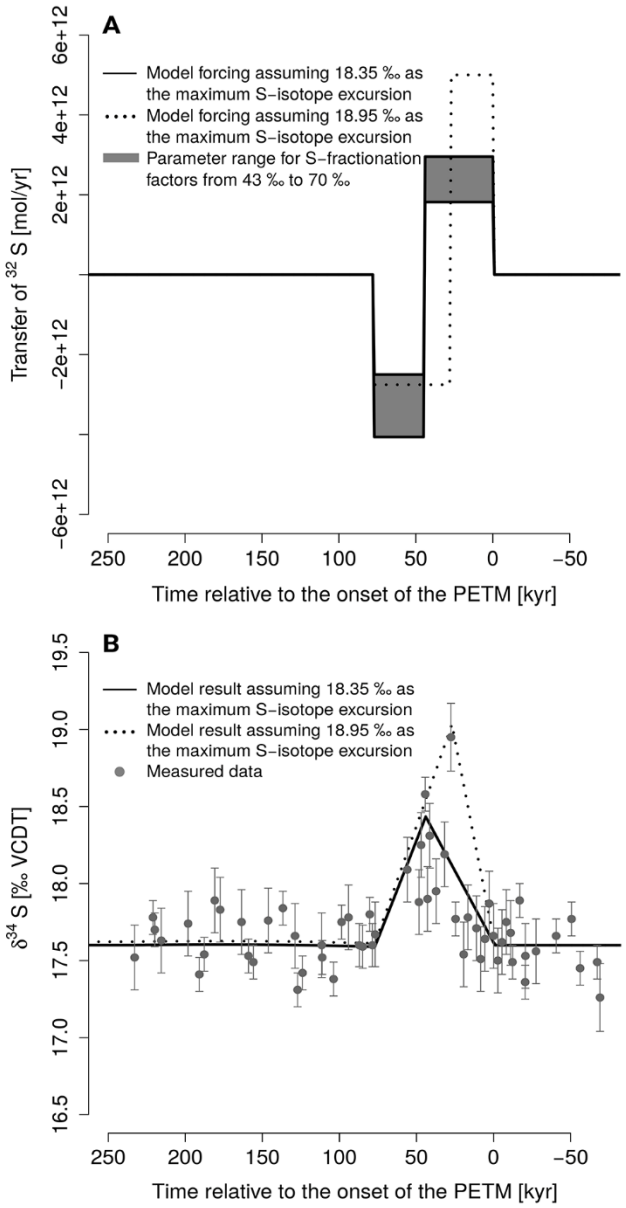

Fig. 2. Model forcing and the resulting S-isotope ratios versus measured data. (**A**) Transfer of ^{32}S in and out of the OMZ. (**B**) Resulting changes in the marine sulfate $\delta^{34}S$ across the PETM. See Supplementary Materials for full model results. Note that in order to model the peak at 18.95‰, we have to adjust the timing of the flux changes.

Downloaded from http://science.sciencemag.org/ on July 19, 2018

Science

Large-scale ocean deoxygenation during the Paleocene-Eocene Thermal Maximum

Weiqi Yao, Adina Paytan and Ulrich G. Wortmann

published online July 19, 2018

ARTICLE TOOLS http://science.sciencemag.org/content/early/2018/07/18/science.aar8658

SUPPLEMENTARY MATERIALS http://science.sciencemag.org/content/suppl/2018/07/18/science.aar8658.DC1

REFERENCES This article cites 51 articles, 15 of which you can access for free
http://science.sciencemag.org/content/early/2018/07/18/science.aar8658#BIBL

PERMISSIONS http://www.sciencemag.org/help/reprints-and-permissions

Use of this article is subject to the Terms of Service

Science (print ISSN 0036-8075; online ISSN 1095-9203) is published by the American Association for the Advancement of Science, 1200 New York Avenue NW, Washington, DC 20005. 2017 © The Authors, some rights reserved; exclusive licensee American Association for the Advancement of Science. No claim to original U.S. Government Works. The title *Science* is a registered trademark of AAAS.

Downloaded from http://science.sciencemag.org/ on July 19, 2018